HHS Public Access

Author manuscript

J Thromb Haemost. Author manuscript; available in PMC 2019 November 01.

Published in final edited form as:

J Thromb Haemost. 2018 November ; 16(11): 2246–2257. doi:10.1111/jth.14288.

Re-evaluation of Mouse Tissue Factor Pathway Inhibitor and Comparison of Mouse and Human Tissue Factor Pathway Inhibitor Physiology

Thomas J. Girard[*], **Kristin Grunz**[*], **Nina M. Lasky**[*], **James P. Malone**[†], and **George J. Broze Jr.**[*]

[*]Division of Hematology, Department of Medicine, Washington University School of Medicine, St. Louis, MO

[†]Proteomics Core Laboratory, Institute of Clinical and Translational Sciences, Washington University School of Medicine, St. Louis, MO

SUMMARY

Background: Mouse models can provide insight into the pathophysiology of human thrombosis and hemostasis. Tissue factor pathway inhibitor (TFPI) regulates coagulation through protein S (PS)-enhanced factor (F)Xa inhibition and FXa-dependent inhibition of FVIIa/tissue factor (TF) activity. TFPI is expressed as isoforms α and β in man, and α, β and γ in the mouse.

Objective: Assess the reliability of extending TFPI-related studies in mice to humans.

Method: Compare mouse and human TFPI physiology using a variety of methods.

Results: Mouse and human TFPI are similar in regard to: 1) the mechanisms for FVIIa/TF and FXa inhibition; 2) TFPIα is a soluble form and TFPIβ is glycosyl phosphatidyl inositol (GPI) membrane anchored; 3) The predominant circulating form of TFPI in plasma is lipoprotein-associated; 4) Low levels of TFPIα circulate in plasma and increase following heparin treatment; and 5) TFPIα is the isoform in platelets. They differ in that: 1) Mouse TFPI circulates at an ×20-fold higher concentration; 2) Mouse lines with isolated isoform deletions show this circulating mouse TFPI is derived from TFPIγ; 3) Sequences homologous to the mouse TFPIγ exon are present in many species, including man, but in primates are unfavorable for splicing; and 4) Tandem mass spectrometry (MS/MS) detects sequences for TFPI isoforms α and β in human plasma and α and γ in mouse plasma.

Conclusion: To dissect the pathophysiological roles of human TFPIα and TFPIβ, studies in TFPIγ null mice, expressing only α and β, only α or only β should better reflect the human situation.

Correspondence: George J. Broze, Jr., Division of Hematology, Campus Box 8125, 660 S. Euclid Ave., St. Louis, MO, 63110, USA. Tel.: 314-362-8811; Fax: 314-362-8826; gbroze@wustl.edu.

ADDENDUM

T.J. Girard, K. Gruntz, N.M. Lasky, and G.J. Broze performed the experiments; J.P. Malone evaluated the MS/MS data; T. Girard and G.J. Broze wrote the manuscript.

DISCLOSURE OF CONFLICT OF INTEREST

G.J. Broze has served as a consultant for Bayer, Pfizer and Portola. The other authors state that they have no conflict of interest.

Keywords

Thrombosis; Hemostasis; Mice; Protein Isoforms; Alternative Splicing

INTRODUCTION

Upon vascular injury, tissue factor (TF) binds plasma Factor (F) VII(a). The FVIIa/TF complex catalytically activates FIX and Factor (F)X leading to the generation of thrombin and a fibrin clot. Beyond coagulation, FVIIa/TF triggers cell-signaling events through protease-activated receptors (PARs),[1,2] which impact the pathophysiology of numerous diseases.[3–9] Tissue factor pathway inhibitor (TFPI) is the major endogenous regulator of FVIIa/TF activity. Through alternative RNA splicing, TFPIα and TFPIβ isoforms are expressed in man and mouse.[10–13] Transcripts for a third form, TFPIγ, have been described in the mouse.[14] All TFPI isoforms contain the same N-terminus followed by two Kunitz-type protease inhibitor domains (K1K2); TFPIα contains a K3 domain and basic C-terminal region;[10] TFPIβ contains a sequence that directs the attachment of a GPI membrane anchor[11,15] and mouse TFPIγ contains a short, unique C-terminal region.[14]

Human TFPI (hTFPI) limits FVIIa/TF activity through formation of a FVIIa/TF/FXa/TFPI quaternary complex[16–20] where K1 binds and inhibits FVIIa and K2 binds FXa; the K3 of hTFPIα lacks protease inhibitory activity.[21] hTFPI K2 also directly inhibits FXa[22] in a process that also involves an epitope within the K1 domain[23–27] and that for hTFPIα is dramatically enhanced by PS (binding to K3) at phospholipid surfaces.[28,29] hTFPIβ, situated at the phospholipid surface of cells, inhibits FVIIa/TF and FXa well in the absence of PS.[30,31]

Mouse models can provide insight into human physiology and disease, including abnormalities concerning hemostasis and thrombosis. In the case of TFPI, these studies have largely focused on sites of TFPI expression (e.g. endothelium and hematopoietic cells) using mouse strains with TFPIK1(−) disrupted genes.[32–38] Knowledge is lacking with respect to the roles each TFPI isoform plays *in vivo* and potential differences between the TFPI physiology in mice and man. Here we report studies using TFPI isoform-specific deleted mice that elucidate similarities and important distinctions between the physiology of TFPI in humans and mice.

METHODS

Mice.

The Washington University Animal Studies Committee approved all mouse studies. Control and CRISPR/Cas9 derived mouse lines were in a C57Bl/6N (B6, Taconic Biosciences) genetic background and FVIIIKO (B6;129S-F8^{tm1Kaz}/J, Jackson Laboratories) mice in a C57Bl/6J-129S4/SvJae genetic background. Littermate TFPI(+/+)/FVIIIKO and TFPIα(−/−)/FVIIIKO mice were generated by mating TFPIα(+/−)/FVIIIKO animals.

Anti-mTFPI160 polyclonal IgG.

Recombinant mTFPI160 (mature amino acids 1–160) was expressed and isolated using the pMAL system (New England Biolabs) and used to raise rabbit anti-mTFPI160 polyclonal IgG that was purified by protein A affinity (Captiva-PriMAB, Repligen) chromatography. Control, pre-immune rabbit IgG was isolated in the same manner.

mTFPI ELISAs.

Two assays, which used the same mTFPI standard (R&D Systems) and produced consistent results, were used: the mTFPI DuoSet ELISA (R&D Systems) and an assay that uses anti-mTFPI160 IgG for capture and anti-mTFPI160 IgG-HRP conjugated (Lighting Link, Innova Biosciences) for detection.

Expression of recombinant (r) proteins.

Mouse cDNAs were from Origene Technologies; mutants were produced by PCR-directed mutagenesis. A pcDNA3.4 vector was use to express rmTFPI (mature amino acids 1–157) wild-type (WT) and rmTFPI's K1(K32I) and K2(R103L) containing mutations at their critical P^1 residues, rmTF, rmFX, and rmFVII in the Expi293 system (Thermo Fisher). ELISA quantified rmTFPI levels. Cells expressing rmTF were lysed by a freeze-thaw cycle in PBS + 5 mM EDTA; membranes isolated by centrifugation (10,000g, 10 min), suspended in PBS and stored frozen. rmTF, rmFVII and rmFX were measured in clotting assays using human normal or factor-deficient plasmas (George King Biomedical). rmFXa was generated by a 30 min incubation of rmFX with 1% (w/w) FX-coagulant protein (XCP, Enzyme Research Laboratories).

Mouse FXa and FVIIa/TF inhibition assays.

Reactions were conducted using proteins in serum-free media. For mFXa assays, rmFXa (1.4 nM final) was pre-incubated with rmTFPIs (0–20 nM final) in 180 uL HSA (100 mM NaCl, 2 mg/mL bovine serum albumin, 20 mM Hepes, pH 7.2) for 20 min. followed by the addition of 20 uL of 2 mM CS1165 substrate (Biophen). For mFVIIa/TF assays, excess mTF, mFVII (50 pM final), and mTFPIs (0–2 nM final) in 160 uL HSA + 5 mM $CaCl_2$ were mixed followed by the addition of 40 uL of mFX (1.4 nM in final volume) with 1 mM CS1165.

Mouse thrombin generation assay.

Pooled, citrated C57Bl/6 mouse plasma was from Innovative Research. Individual mouse plasmas were prepared by centrifugation (5,000 g × 15 min) of blood drawn from the inferior vena cava into 1/9 volume of 3.8% sodium citrate. Corn trypsin inhibitor (CTI, Enzyme Research Laboratories) was added to 12.5 ug/mL. Plasma (20 uL) was incubated for 30 min with 40 uL HSA containing 50 ug/mL CTI without or with theses other reagents: mTFPIα (R&D Systems); anti-hPS antibody (#A0384, Dako); and anti-mTFPI160. Next was added 20 uL of 60 ug/mL rabbit brain cephalin (Pentapharm) containing the specified concentration of mTF [from a mouse brain saline extract, mTF assayed by ELISA (Abcam)]. Reactions were initiated by adding 20 uL of 1 mM Z-GGR-AMC (Sigma-Aldrich) in 50 mM $CaCl_2$. Data were collected using a Fluoroskan Ascent instrument and analyzed as

described.[39] Note that the anti-hPS antibody used in these studies reportedly cross-reacts with mPS, but the potency of its inhibition of mPS has not been established,[40,41] and that the rmTFPIα(1–259) reagent lacks the distal C-terminus domain, which is required for optimal FXa inhibition in the human system [29,42].

Bovine FXa ligand and western blotting were performed as described.[15]

Mouse platelet isolation.

Blood obtained with heparinized capillary tubes from the retro-orbital plexus of 5–10 mice was pooled, mixed gently with 3 volumes BSGCe (116 mM NaCl, 8.6 mM Na_2HPO_4, 1.6 mM KH_2PO_4, 13.6 mM sodium citrate, 11.1 mM glucose, 0.9 mM Na_2EDTA, pH 6.8) and placed in a 15 mL conical tube. The mixture was underlayed with an equal volume of OptiPrep 5/22 [5 volumes of OptiPrep (Sigma-Aldrich); mixed with 22 volumes 0.145 M NaCl, 0.02 M Hepes, 1 mM EDTA, pH 7.4] with a specific gravity of 1.063. The tube was centrifuged at 350 g for 15 min. at RT. Approximately 50% of the cloudy Optiprep 5/22 layer above the visible RBC/WBC pellet was collected; this was mixed 1:1 with BSGCe and centrifuged at 1000 g for 15 min. to pellet the platelets. Platelets were gently washed twice with BSGCe, suspended and counted (Hemavet; Drew Scientific). Platelets were lysed with 30 mM CHAPS, centrifuged at 16,000 g × 10 min., and supernatant TFPI determined by ELISA.

Cab-O-Sil adsorption of lipoproteins.

To 1 mL of C57Bl/6 mouse plasma (Innovative Research) was added 1 mL of HS (100 mM NaCl, 20 mM Hepes, pH 7.4) or 1 mL of HS containing 50 mg/mL Cab-O-Sil M5 fumed silica (Eastman Kodak). After mixing by rotation overnight at 4°C, samples were centrifuged at 16,000 g for 15 min., the supernatants passed through 0.22 um filters, and their TFPI concentrations measured by ELISA.

Density ultracentrifugation of lipoproteins.

To 3 mL of C57Bl/6 mouse plasma was added 30 uL 250 mM EDTA and 1 g of KBr (final density 1.21 g/mL). A portion (2.5 mL) of the mixture was centrifuged in an SW55Ti rotor at 50,000 rpm for 48 hours at 4°C. Samples (0.5 mL) from the top and the bottom of the tube were dialyzed against 0.1 M NaCl, 0.02 M Hepes, 5 mM EDTA, and their mTFPI concentrations determined by ELISA.

Identification of TFPIγ exon orthologs.

Using EMBL-EBI ClustalW2 mouse TFPIγ exon sequence was aligned with the human, rat, rabbit, cat, and dog TFPI genes to identify orthologs; rat γ exon encoding sequence was used to identify squirrel and Chinese hamster orthologs; and human γ exon homolog DNA sequence was used to identify other primate orthologs. NCBI TFPI gene RNA-seq intron features were used to identify TFPIγ exon splicing.

Identification of human γ sequence in 3’ untranslated TFPIβ message.

Human RNAs from 20 tissues (Clontech panel #636643); were reverse transcribed (Super Script III, Invitrogen) followed by PCR amplification using a K2 domain encoding forward

primer and a γ exon reverse primer (see Table 1). Products were analyzed by agarose gel electrophoresis and sequenced.

Purification of mouse TFPI from plasma.

Total plasma TFPI was isolated from 100 mL of citrated C57Bl/6 mouse plasma with 10 mL protease inhibitor cocktail (#2714, Sigma-Aldrich). Plasma was rocked overnight at 4°C with 4 mL of Affigel-10-linked (BioRad) rabbit anti-mTFPI160 IgG (5 mg IgG/mL Affigel-10). The plasma/Affigel slurry was poured into a column; washed with 30 volumes of 0.5 M NaCl in TSE (5 mM EDTA, 20 mM Tris, pH 7.4). Bound mTFPI was eluted with 0.02 M glycine, pH 2.5, adjusted to pH 7.4 with Tris (1.0 M, pH 8.3), and dialyzed into 0.15 M NaCl in TSE.

To isolate mouse lipoprotein-associated TFPI, three batches of 30 mL of citrated C57Bl/6 mouse plasma with 3 mL protease inhibitor cocktail were passed over a 3 × 180 cm Sephacryl 300 column (GE Healthcare) equilibrated and eluted with 0.5 M NaCl in TSE. Fractions containing the major TFPI peak were pooled and further purified using the anti-mTFPI160 IgG Affigel-10 column procedure described above.

Purification of human TFPI from plasma.

Total plasma TFPI was isolated from 100 mL of human plasma (Red Cross) with 10 mL protease inhibitor cocktail. The plasma was filtered (0.45 um) and then rocked overnight at 4°C with 4 mL of Affigel-10-linked anti-hTFPI 2H8 Mab (5 mg IgG/mL Affigel-10). The plasma/Affigel slurry was poured into a column and the hTFPI isolated using a similar procedure as that described above for the anti-mTFPI160 IgG Affigel-10 column.

Tandem mass spectroscopy (MS/MS) analysis.

TFPI samples were digested with Lys-C, Lys-C and trypsin or Glu-C by conventional methods and analyzed using Mascot version 2.3.02 (Matrix Science). Scaffold version 4.0.5 (Proteome Software Inc.) was used to validate MS/MS based peptide and protein identifications. Peptides (≥ 5 residues) were established at greater than 90% probability (Protein Prophet TM algorithm).

Detection of phosphatidylinositol-specific phospholipase C (PIPLC) releasable mTFPI from mouse organs.

Membranes were prepared as described[15] from organs harvested from mice that had been perfused with 20 mL of PBS containing 5 mM EDTA and 5 units per ml of heparin (Sagent Pharmaceuticals). Membrane protein content was determined by the Bradford method. Membranes were treated without or with PIPLC (30 units/mL final) in HS containing 10% protease inhibitor cocktail for 1 hour followed by a 10 min. centrifugation at 13,000 g. ELISA was used to measure mTFPI in the supernatants.

Generation of exon-specific knockout mice.

CRISPR/Cas9 technology[43] was used to create TFPI exon-specific deletions, or γ intron/exon splice site destruction. Sequences flanking the isoform specific exon deletions and γ

spliced site disruption are shown in Table 2. Genotyping of mice was performed using the PCR Blood Phusion mix (#547L Thermo-Fisher). Reaction conditions were 98°C for 2 min × 1 cycle; 98°C for 15 sec, 68°C for 30 sec, 72°C for 30 sec × 30 cycles; and 72°C for 2 min × 1 cycle. PCR products were analyzed by agarose gel electrophoresis. Primers (Integrated DNA Technologies) used to identify wild type and exon-deletions are summarized in Table 1.

Quantitative PCR of mTFPI isoform transcripts.

RNA was isolated from mouse organs as described.[44] Samples were analyzed by one-step RT-PCR using Path-ID RT-PCR kit #4388639 (Ambion) and standard conditions with an annealing temperature of 65°C. Individual reactions were run for each isoform using the FAM-probe and primers listed in Table 1 and with the β-actin control (#4352933E; Applied Biosystems) using the Applied Biosystems StepOnePlus Real-Time PCR system. Data were analyzed by the Livak method.[45]

RESULTS

Structure/function analysis of mTFPI.

To determine if the Kunitz domains in mouse and human TFPI function similarly, the abilities of truncated rmTFPI(1–157) WT and forms containing mutated K1 or K2 P^1 residues to bind to and inhibit mFXa and to inhibit mFVIIa/mTF activity in the presence of mFX(a) were assessed. WT and K1-mutated rmTFPI inhibited rmFXa similarly and bound HRP-labeled bovine FXa on a ligand blot (Figure 1A, B, and G). Mouse K2 mutated rmTFPI did not inhibit rmFXa activity and did not recognize bovine FXa on ligand blot (Figure 1C and G). WT rmTFPI inhibited mouse rmFVIIa/rmTF activity (Figure 1D), but the K1-mutated and K2-mutated rmTFPIs each failed to significantly inhibit rmFVIIa/rmTF activity (Figure 1E and F). These results indicate that, like man, the second Kunitz domain in mTFPI is responsible for the binding to and inhibiting FXa and that, in a FXa-dependent manner, the first Kunitz domain of mTFPI is responsible for inhibition of FVIIa/TF. An effect of anti-hPS antibodies in TF-induced thrombin generation assays could only be detected following the addition of rmTFPIα (Figure 1H). These data, however, demonstrate that mPS enhances the anticoagulant activity of mTFPIα, as is the case for the human proteins.

Characterization of mouse plasma TFPI.

The major form of mouse plasma TFPI migrates on SDS-PAGE as a ×41 kDa protein, but elutes from size-exclusion column chromatography at an apparent molecular weight of ×270 kDa (Figure 2A) suggesting that, like hTFPI, it may be bound to lipoprotein (HDL is the predominant lipoprotein in the mouse plasma). Consistent with this notion, >98% of the TFPI in mouse plasma binds to fumed silica (Cab-O-Sil), which binds lipoproteins avidly.[46] Following ultracentrifugation of mouse plasma in a KBr solution of density 1.21 g/mL, in which lipoproteins float,[47] the concentration of TFPI in the top 20% of the sample was 57-fold greater than the concentration of TFPI in the bottom 20% of the sample.

The major form of mTFPI in plasma was isolated by size exclusion chromatography followed by anti-mTFPI immunoaffinity chromatography. MS/MS analysis of this "lipoprotein-associated" mTFPI identified it as a two Kunitz (K1K2) domain form lacking detectible C-terminal isoform-specific sequences (Figure 2B). This result is similar to lipoprotein-associated hTFPI, which also appears to be a C-terminal truncated, two-Kunitz (K1K2) domain form.[48] MS/MS analysis of total TFPI isolated from mouse plasma, detected both mTFPIα-specific and mTFPIγ-specific peptides, but no TFPIβ-specific peptides (Figure 2B). MS/MS analysis of total hTFPI from human plasma demonstrated TFPIα- and TFPIβ-specific peptides (Figure 2C).

TFPIγ exon orthologs.

The TFPIγ-exon DNA sequence was reported to be unique to the mouse.[14] Selectively searching the TFPI genes revealed that sequences homologous with the mouse γ exon are indeed present within the TFPI gene of many species, including man (Table 3). NCBI databases contain no human transcripts with this sequence. Using appropriate primers and RT-PCR messages from numerous human tissues were found to contain this TFPIγ homologous sequence but, in every case it was part of TFPIβ 3'-untranslated message, never an exon (data not shown). Of note, the 3' splice acceptor sequence for the TFPIγ exon in mouse, rat, Chinese hamster, squirrel and rabbit is CAG, which is commonly used for splicing (71%); the corresponding splice sequence in man and other primates, GAG, is rarely utilized (<1%) for splicing (Table 3).[49] NCBI TFPI gene RNA-seq intron features identified TFPIγ exon splicing in mouse, rat, and hamster, but not in rabbit, cat, dog or primates (data was insufficient to evaluate squirrel).

Mouse TFPI isoform transcripts.

TFPI α exon-deleted, β exon-deleted, β/γ exons-deleted and γ exon-disrupted mouse strains were generated using CRISPR/Cas9 technology. The KO mice, born at or near Mendelian ratios (Table 4), appear healthy and reproduce.

TFPI isoform transcript selective amplification was achieved by using a common upstream primer and isoform specific primers that span their respective exon/exon splice sites (Figure 3A-C). Among six organs analyzed, the relative level of γ message ranged from 40–65%, α message ranged from 30–50% and the level of β message was ×10% of total TFPI message (Figure 3D-I).

Mouse TFPI isoform proteins.

Two distinct mouse TFPI ELISAs showed TFPI in mouse plasma circulates at ×20 times the level in man and is not detectably affected by heparin treatment: 31.5 ± 3.7 nM before and 29.7 ± 4.1 nM (n=10) 15 min after 2 units of heparin (IP). Plasma mTFPI levels in TFPIα(−/−) and TFPIβ(−/−) mice are similar to WT mice (×100%). They are ×50% in TFPIγ(+/−) and TFPIβ/γ(+/−) mice and ≤2% in TFPIγ(−/−) and TFPIβ/γ(−/−) mice (Figure 4A). Thus, the major form of mouse plasma TFPI is derived from mTFPIγ, not α or β.

Studies of mice with combined TFPIβ/γ(−/−) gene deletion (expressing α only) show a plasma level of TFPIα of 66.8 ± 12.9 pM that increases 7.3 ± 2.5-fold after heparin

treatment (Figure 4B). These baseline TFPIα measurements represent a total value and the distribution of TFPIα derived "free" and lipoprotein-associated forms, if any, remains to be determined. Four individual experiments using platelets isolated from 5–10 mice, showed the level of TFPI in platelets (at 850,000/uL) in wild-type mouse blood was 74.6 ± 16.0 pM. Platelet TFPI is absent in TFPIα KO mice, confirming a previous study [50] that in mice, like humans, platelet TFPI is TFPIα (Figure 4C).

Membranes isolated from tissues of WT, β KO, γ KO and β/γ KO mice were treated without or with PIPLC and the released TFPI measured by ELISA (Figure 4D). PIPLC treatment released TFPI from WT membranes, whereas, membranes from TFPIβ KO and TFPIβ/γ KO mice show no significant release of TFPI with PIPLC treatment. These results are consistent with TFPIβ being the predominant GPI-anchored isoform. Of interest, deletion of the γ exon results in a significant ×2.7-fold increase in PIPLC-releasable TFPIβ. It is plausible that the loss of the γ exon splicing increases RNA splicing to the nearby β exon leading to increased β protein.

Due to its potent PS- and C-terminal-dependent inhibition of FXa, TFPIα plays the paramount anticoagulant role in *in vitro assays* of coagulation in human plasma. Compared to TFPIα, C-terminal truncated forms of recombinant hTFPI and lipoprotein-associated hTFPI containing only K1 and K2, like mouse lipoprotein-associated TFPI, are poor inhibitors of FXa[29,42] and their anticoagulant effect is difficult to detect in plasma coagulation assays, including standard thrombin generation assays [51–53]. To demonstrate that the lipoprotein-associated, C-terminal truncated form of TFPI in mouse plasma possesses relevant anticoagulant activity, the *in vitro* thrombin generation assay was preformed using plasma from mice with hemophilia (FVIIIKO), which reduces the dependence of the results on FXa inhibition. Under these conditions, thrombin generation in the plasma obtained from both TFPIα(+/+)/FVIIIKO and TFPIα(−/−)/FVIIIKO mice was dramatically enhanced by anti-mTFPI160 antibodies (Figure 4E and F).

DISCUSSION

Mouse models have been used extensively to evaluate the role of TFPI in hemostasis and thrombosis. Although mice possess TFPIγ transcripts[14] that are not present in humans, potential differences between TFPI physiology in humans and mice have not been carefully assessed. Such studies have been hampered by the lack of isoform-specific antibodies for each mouse TFPI isoform. Here, a variety of methods, including MS/MS analysis and CRISPR/Cas9 technology to generate mice with specific TFPI isoform deletions have been used to better compare human and mouse TFPI physiology.

A major result of the current work is the demonstration that mouse plasma TFPI, which circulates at a level ×20-fold the level of TFPI in human plasma, is derived predominantly from mTFPIγ, rather than another mTFPI isoform (e.g. mTFPIβ)[54,55] Although mouse TFPIγ exon homologous sequence was reportedly not present in other species,[14] we found TFPIγ orthologs in several species, including man. RNA-seq data indicate the γ exon is used in mouse, rat, and hamsters, but the TFPIγ ortholog sequence in man is not recognized as an exon, perhaps in part due to an unfavorable 3' acceptor splice site sequence.

Matching the hTFPI Kunitz-domain functions,[21] we found that the mTFPI first and second Kunitz domains inhibit FVIIa and FXa, respectively, and that the FVIIa/TF inhibition is dependent on FXa.

In human plasma, the major form of TFPI appears to be C-terminal truncated, two Kunitz domain (K1K2) hTFPI that is associated with lipoproteins, LDL > HDL.[48] Whether the TFPI isoform source for lipoprotein associated human TFPI is hTFPIα, hTFPIβ or both has not been determined. The major form of TFPI circulating at high levels bound to lipoprotein in mouse plasma also appears to be a truncated K1K2 mTFPI form and is derived predominantly from mTFPIγ. The mechanism responsible for the association of hTFPI and mTFPI with plasma lipoproteins is not known.

Human TFPIα circulates in plasma at low levels, which are comparable to the levels of TFPIα carried by platelets in human blood (at ×200,000 platelets/uL).[56] Heparin administration in man increases total hTFPI in plasma 2- to 3-fold due to an ×15-fold increase in hTFPIα, presumably released by endothelial cells.[57–59] It has been reported that mouse TFPIα differs from its human counterpart in that it is not produced by endothelial cells and is not present in plasma.[60] Our MS/MS results however, demonstrate the presence of TFPIα in mouse plasma and, based at least on the results in mice with combined TFPIβ/γ(−/−) gene deletion (expressing α only), mTFPIα circulates in mouse plasma at low levels, which, like in humans, are comparable to the levels of the TFPIα in the platelets in mouse blood (at ×850,000/uL). In contrast to the case in humans, we find that an effect of heparin-induced release of mTFPIα on total mouse plasma TFPI levels is difficult to detect due to the high plasma levels of TFPI derived from TFPIγ. This result differs from a previous report that used a different assay method.[54] In the TFPIβ/γ deleted mice expressing only mTFPIα, however, a several fold-increase in TFPIα can be demonstrated following heparin treatment.

PIPLC treatment, which cleaves GPI-anchored proteins, releases TFPI from cell membranes.[61] For some time it was thought that this represented TFPIα bound to an unidentified, GPI-anchored co-receptor.[62,63] It has since been shown for human placenta and endothelial cells that TFPIβ is the form released from the cell surface by PIPLC.[15] Consistent with the latter finding, PIPLC treatment of membranes from TFPIβ KO and TFPIβ/γ KO mice show no significant release of TFPI in contrast to controls. Thus, mTFPIβ also appears to be the predominant GPI-anchored TFPI isoform in the mouse.

MS/MS analysis demonstrated the presence of peptides from hTFPIα and hTFPIβ in human plasma and from mTFPIα and mTFPIγ in mouse plasma. Our inability to detect mTFPIβ peptides in mouse plasma, however, must be considered cautiously. The amino acid sequence of mTFPIβ is such that its processing to contain a GPI anchor and potential proteolytic shedding from a membrane surface would produce mTFPIβ peptides that would not have been identified under the conditions of our MS/MS analysis.

The availability of TFPIα and combined TFPIβγ KO mice enabled us to validate RT-PCR assays with respect to TFPI isoform specificity. For example, assays for isoform-specific transcripts show no signals in their respective isoform-deleted mice. With these assays, the

levels of TFPIα and TFPIγ transcripts in wild-type mice are roughly similar across tissues (×40–60% each) and TFPIβ message represents ×10% of the total TFPI transcripts. It has been reported that mouse tissues express 5–50 times more TFPIα than TFPIβ and that TFPIγ message is expressed at ×2-fold the level of TFPIβ.[54] The discrepancy between studies may be due to the use of different primers, reagents and assay conditions.

The anticoagulant activity of two-Kunitz (K1K2) domain forms of TFPI is difficult to detect in *in vitro* plasma coagulation assays since, compared to TFPIα, they are poor inhibitors of FXa. The K1K2 forms of TFPI, however, are not inert (Figure 4E) and possess potent anti-FVIIa/TF activity (Figure 1D). Moreover, they likely function *in vivo* since they inhibit FVIIa/TF at cultured cell surfaces and under conditions mimicking vascular flow in a fashion comparable to full-length TFPIα.[64–66]

In sum, the properties of TFPIα and TFPIβ in the mouse appear to mirror those of the same isoforms in humans. Mice differ dramatically from man, however, in that their plasma contains a 20-fold higher level of K1K2, C-terminal truncated TFPI derived from TFPIγ, an isoform not found in man. *In vitro* coagulation assays are an incomplete measure of the overall and isoform-specific pathophysiologic roles of TFPI as they do not detect the potential *in vivo* contributions of vascular flow and endogenous cell-surface associated TFPIβ, nor do they assess potential functional properties of TFPI unrelated to thrombin generation. Here, *in vivo* experimentation is required and TFPIγ gene-deleted mice, expressing only the TFPIα and TFPIβ isoforms, may serve as a more appropriate human surrogate. Moreover, their comparison with mice expressing only mTFPIα and only mTFPIβ in mouse models of hemostasis, thrombosis, inflammation, and cancer/metastasis, etc. could provide insight into the potential differential roles of the TFPI isoforms in these human diseases.

ACKNOWLEDGMENTS

We recognize the Washington University School of Medicine Genomic Engineering and iPC (GEiC) Center for the design and production of the CRISPR reagents and J. Michael White and the Pathology Microinjection Core for production of the TFPI exon deleted mouse strains. The laboratory of Reed Townsend, Washington University, St. Louis, MO, conducted the tandem MS/MS analyses with support from grants UL1 TR000448 and P41GM103422–35. Our work was supported by National Institutes of Health grants HL077193 and HL112303.

REFERENCES

1. Camerer E, Huang W, Coughlin SR. Tissue factor- and factor X-dependent activation of protease-activated receptor 2 by factor VIIa. Proc Natl Acad Sci U S A 2000; 97: 5255–60. [PubMed: 10805786]
2. Riewald M, Ruf W. Mechanistic coupling of protease signaling and initiation of coagulation by tissue factor. Proc Natl Acad Sci U S A 2001; 98: 7742–7. [PubMed: 11438726]
3. Versteeg HH, Ruf W. Emerging insights in tissue factor-dependent signaling events. Semin Thromb Hemost 2006; 32: 24–32. [PubMed: 16479459]
4. Chu AJ. Role of tissue factor in thrombosis. Coagulation-inflammation-thrombosis circuit. Front Biosci 2006; 11: 256–71. [PubMed: 16146730]
5. Rao LV, Pendurthi UR. Tissue factor-factor VIIa signaling. Arterioscler Thromb Vasc Biol 2005; 25: 47–56. [PubMed: 15569823]

6. Sethi AS, Lees DM, Douthwaite JA, Corder R. Factor VIIa stimulates endothelin-1 synthesis in TNF-primed endothelial cells by activation of protease-activated receptor 2. Clin Sci (Lond) 2005; 108: 255–63. [PubMed: 15548135]

7. Muth H, Kreis I, Zimmermann R, Tillmanns H, Holschermann H. Differential gene expression in activated monocyte-derived macrophages following binding of factor VIIa to tissue factor. Thromb Haemost. 2005; 94: 1028–34. [PubMed: 16363246]

8. Uusitalo-Jarvinen H, Kurokawa T, Mueller BM, Andrade-Gordon P, Friedlander M, Ruf W. Role of protease activated receptor 1 and 2 signaling in hypoxia-induced angiogenesis. Arterioscler Thromb Vasc Biol 2007; 27: 1456–62. [PubMed: 17363687]

9. Pawlinski R, Pedersen B, Schabbauer G, Tencati M, Holscher T, Boisvert W, Andrade-Gordon P, Frank RD, Mackman N. Role of tissue factor and protease-activated receptors in a mouse model of endotoxemia. Blood 2004; 103: 1342–7. [PubMed: 14576054]

10. Wun TC, Kretzmer KK, Girard TJ, Miletich JP, Broze GJ, Jr. Cloning and characterization of a cDNA coding for the lipoprotein-associated coagulation inhibitor shows that it consists of three tandem Kunitz-type inhibitory domains. J Biol Chem 1988; 263: 6001–4. [PubMed: 2452157]

11. Zhang J, Piro O, Lu L, Broze GJ, Jr. Glycosyl phosphatidylinositol anchorage of tissue factor pathway inhibitor. Circulation 2003; 108: 623–7. [PubMed: 12835228]

12. Chang JY, Monroe DM, Oliver JA, Liles DK, Roberts HR. Cloning, expression, and characterization of mouse tissue factor pathway inhibitor (TFPI). Thromb Haemost 1998; 79: 306–9. [PubMed: 9493581]

13. Chang JY, Monroe DM, Oliver JA, Roberts HR. TFPIbeta, a second product from the mouse tissue factor pathway inhibitor (TFPI) gene. Thromb Haemost 1999; 81: 45–9. [PubMed: 9974373]

14. Maroney SA, Ferrel JP, Collins ML, Mast AE. Tissue factor pathway inhibitor-gamma is an active alternatively spliced form of tissue factor pathway inhibitor present in mice but not in humans. J Thromb Haemost 2008; 6: 1344–51. [PubMed: 18503630]

15. Girard TJ, Tuley E, Broze GJ, Jr. TFPIbeta is the GPI-anchored TFPI isoform on human endothelial cells and placental microsomes. Blood 2012; 119: 1256–62. [PubMed: 22144186]

16. Girard TJ, Broze GJ, Jr. Tissue factor pathway inhibitor. Methods in Enzymology 1993; 222: 195–209. [PubMed: 8412794]

17. Hubbard AR, Jennings CA. Inhibition of tissue thromboplastin-mediated blood coagulation. Thromb Res 1986; 42: 489–98. [PubMed: 3087014]

18. Sanders NL, Bajaj SP, Zivelin A, Rapaport SI. Inhibition of tissue factor/factor VIIa activity in plasma requires factor X and an additional plasma component. Blood 1985; 66: 204–12. [PubMed: 3873968]

19. Rao LV, Rapaport SI. Studies of a mechanism inhibiting the initiation of the extrinsic pathway of coagulation. Blood 1987; 69: 645–51. [PubMed: 3492226]

20. Broze GJ, Jr., Miletich JP Characterization of the inhibition of tissue factor in serum. Blood 1987; 69: 150–5. [PubMed: 3024756]

21. Girard TJ, Warren LA, Novotny WF, Likert KM, Brown SG, Miletich JP, Broze GJ, Jr. Functional significance of the Kunitz-type inhibitory domains of lipoprotein-associated coagulation inhibitor. Nature 1989; 338: 518–20. [PubMed: 2927510]

22. Broze GJ, Jr, Warren LA, Novotny WF, Higuchi DA, Girard JJ, Miletich JP. The lipoprotein-associated coagulation inhibitor that inhibits the factor VII-tissue factor complex also inhibits factor Xa: insight into its possible mechanism of action. Blood 1988; 71: 335–43. [PubMed: 3422166]

23. Higuchi D, Wun T-C, Likert KM, Broze GJ, Jr. The effect of leukocyte elastase on tissue factor pathway inhibitor. Blood 1992; 79: 1712–9. [PubMed: 1558967]

24. Petersen LC, Bjorn SE, Nordfang O. Effect of leukocyte proteinases on tissue factor pathway inhibitor. Thrombosis Haemost 1992; 67: 537–41.

25. Peraramelli S, Suylen DPL, Rosing J, Hackeng TM. The Kunitz1 and Kunitz 3 domains of tissue factor pathway inhibitor are required for efficient inhibition of factor Xa. Thromb Haemost 2012; 108: 266–76. [PubMed: 22627666]

26. Dockal M, Hartmann R, Fries M, Thomassen MC, Heinzmann A, Ehrlich H, Rosing J, Osterkamp F, Polakowski T, Reineke U, Griessner A, Brandstetter H, Scheiflinger F. Small peptides blocking

inhibition of factor Xa and tissue factor-factor FVIIa by tissue factor pathway inhibitor (TFPI). J Biol Chem 2014; 289: 1732–41. [PubMed: 24275667]

27. Augustsson C, Svensson A, Kjaer B, Chao T- Y, Wenjuan X, Krogh BO, Breinhot J, Clausen JT, Hilden I, Petersen HH, Petersen LC. Factor Xa and VIIa inhibition by tissue factor pathway inhibitor is prevented by a monoclonal antibody to its Kunitz-1 domain. J Thromb Haemost 2018; 16: 893–4. [PubMed: 29532595]
28. Hackeng TM, Sere KM, Tans G, Rosing J. Protein S stimulates inhibition of the tissue factor pathway by tissue factor pathway inhibitor. Proc Natl Acad Sci U S A 2006; 103: 3106–11. [PubMed: 16488980]
29. Ndonwi M, Tuley EA, Broze GJ, Jr. The Kunitz-3 domain of TFPI-alpha is required for protein S-dependent enhancement of factor Xa inhibition. Blood 2010; 116: 1344–51. [PubMed: 20479289]
30. Piro O, Broze GJ, Jr. Comparison of cell-surface TFPIalpha and beta. J Thromb Haemost 2005; 3: 2677–83. [PubMed: 16246254]
31. Wood JP, Ellery PE, Maroney SA, Mast AE. Protein S is a cofactor for platelet and endothelial tissue factor pathway inhibitor-alpha but not for cell surface-associated tissue factor pathway inhibitor. Arterioscler Thromb Vasc Biol 2014; 34: 169–76. [PubMed: 24233490]
32. Huang ZF, Higuchi D, Lasky N, Broze GJ, Jr. Tissue factor pathway inhibitor gene disruption produces intrauterine lethality in mice. Blood 1997; 90: 944–51. [PubMed: 9242522]
33. Maroney SA, Cooley BC, Ferrel JP, Bonesho CE, Nielsen LV, Johansen PB, Hermit MB, Petersen LC, Mast AE. Absence of hematopoietic tissue factor pathway inhibitor mitigates bleeding in mice with hemophilia. Proc Natl Acad Sci U S A 2012; 109: 3927–31. [PubMed: 22355108]
34. White TA JT, Zarzhevsky N, Tom C, Delacroix S, Holroyd EW, Maroney SA, Singh R, Pan S, Fay WP, van Deursen J, Mast AE, Sandhu GS, Simari RD. Endothelial-derived tissue factor pathway inhibitor regulates arterial thrombosis, but is not required for development or hemostasis. Blood 2010; 116: 1787–94. [PubMed: 20516367]
35. Wang J, Xiao J, Wen D, Wu X, Mao Z, Zhang J, Ma D. Endothelial cell-anchored tissue factor pathway inhibitor regulates tumor metastasis to the lung in mice. Mol Carcinog 2016; 55: 882–96. [PubMed: 25945811]
36. Eitzman DT, Westrick RJ, Bi X, Manning SL, Wilkinson JE, Broze GJ, Ginsburg D. Lethal perinatal thrombosis in mice resulting from the interaction of tissue factor pathway inhibitor deficiency and factor V Leiden. Circulation 2002; 105: 2139–42. [PubMed: 11994245]
37. Westrick RJ, Bodary PF, Xu Z, Shen YC, Broze GJ, Eitzman DT. Deficiency of tissue factor pathway inhibitor promotes atherosclerosis and thrombosis in mice. Circulation 2001; 103: 3044–6. [PubMed: 11425765]
38. Singh R, Pan S, Mueske CS, Witt TA, Kleppe LS, Peterson TE, Caplice NM, Simari RD. Tissue factor pathway inhibitor deficiency enhances neointimal proliferation and formation in a murine model of vascular remodelling. Thromb Haemost 2003; 89: 747–51. [PubMed: 12669131]
39. Hemker HC, Kremers R. Data management in thrombin generation. Thromb Res 2013; 131: 3–11. [PubMed: 23158401]
40. Saller F, Brisset AC, Tchaikovski SN, Azevedo M, Chrast R, Fernandez JA, Schapira M, Hackeng TM, Griffin JH, Angelillo-Scherrer A. Generation and phenotypic analysis of protein S-deficient mice. Blood 2009; 114: 2307–14. [PubMed: 19567881]
41. Prince R, Bologna L, Manetti M, Melchiorre D, Rosa I, Dewarrat N, Suardi S, Amini P, Fernandez JA, Burnier L, Quarroz C, Reina Caro MD, Matsumura Y, Kremer Hovinga JA, Griffin JH, Simon HU, Ibba-Manneschi L, Saller F, Calzavarini S, Angelillo-Scherrer A. Targeting anticoagulant protein S to improve hemostasis in hemophilia. Blood 2018; 131: 1360–71. [PubMed: 29317453]
42. Wesselschmidt R, Likert K, Huang Z, MacPhail L, Broze GJ, Jr. Structural requirements for tissue factor pathway inhibitior interactions with factor Xa and heparin. Blood Coagul Fibrinolysis 1993; 4: 661–9. [PubMed: 8292716]
43. Parikh BA, Beckman DL, Patel SJ, White JM, Yokoyama WM. Detailed phenotypic and molecular analyses of genetically modified mice generated by CRISPR-Cas9-mediated editing. PloS One 2015; 10: e0116484. [PubMed: 25587897]

44. Girard TJ, Lasky NM, Tuley EA, Broze GJ, Jr. Protein Z, protein Z-dependent protease inhibitor (serpinA10), and the acute-phase response. J Thromb Haemost 2013; 11: 375–8. [PubMed: 23205927]
45. Livak KJ, Schmittgen TD. Analysis of relative gene expression data using real-time quantitative PCR and the 2(-Delta Delta C(T)) method. Methods 2001; 25: 402–8. [PubMed: 11846609]
46. Weinstein DB. A single step adsorption method for the removal of lipoproteins and preparation of cholesterol-free serum. Circulation 1979; 60(Suppl 2): 54, Abstract 160.
47. Rosales C, Gillard BK, Courtney HS, Blanco-Vaca F, Pownall HJ. Apolipoprotein modulation of streptococcal serum opacity factor activity against human plasma high-density lipoproteins. Biochemistry 2009; 48: 8070–6. [PubMed: 19618959]
48. Broze GJ, Jr., Lange GW, Duffin KL, MacPhail L. Heterogeneity of plasma tissue factor pathway inhibitor. Blood Coagul Fibrinolysis 1994; 5: 551–9. [PubMed: 7841311]
49. Zhang MQ. Statistical features of human exons and their flanking regions. Hum Mol Genet 1998; 7: 919–32. [PubMed: 9536098]
50. Maroney SA, Cooley BC, Ferrel JP, Bonesho CE, Mast AE. Murine hematopoietic cell tissue factor pathway inhibitor limits thrombus growth. Arterioscler Thromb Vasc
51. Dahm AEA, Andersen TO, Rosendaal F, Sandset PM. A novel anticoagulant activity assay of tissue factor pathway inhibitor I (TFPI). J Thromb Haemost 2005; 3: 651–8. [PubMed: 15842349]
52. Hansen JB, Huseby KR, Huseby NE, Ezban M, Nordoy A. Tissue factor pathway inhibitor in complex with low density lipoprotein isolated from human plasma does not possess anticoagulant function in tissue factor-induced coagulation in vitro. Thromb Res 1997; 85: 413–25. [PubMed: 9076898]
53. Winckers K, Thomassen S, ten Cate H, Hackeng TM. Platelet full length TFPI-α in healthy volunteers is not affected by sex or hormone use. PLoS One 2017; 12: e0168273. [PubMed: 28158181]
54. Maroney SA, Ferrel JP, Pan S, White TA, Simari RD, McVey JH, Mast AE. Temporal expression of alternatively spliced forms of tissue factor pathway inhibitor in mice. J Thromb Haemost 2009; 7: 1106–13. [PubMed: 19422457]
55. Wood JP, Ellery PE, Maroney SA, Mast AE. Biology of tissue factor pathway inhibitor. Blood 2014; 123: 2934–43. [PubMed: 24620349]
56. Novotny WF, Girard TJ, Miletich JP, Broze GJ, Jr. Platelets secrete a coagulation inhibitor functionally and antigenically similar to the lipoprotein associated coagulation inhibitor. Blood 1988; 72: 2020–5. [PubMed: 3143429]
57. Sandset PM, Abildgaard U, Larsen ML. Heparin induces release of extrinsic coagulation pathway inhibitor (EPI). Thromb Res 1988; 50: 803–13. [PubMed: 3413731]
58. Novotny WF, Palmier M, Wun TC, Broze GJ, Jr., Miletich JP. Purification and properties of heparin-releasable lipoprotein-associated coagulation inhibitor. Blood 1991; 78: 394–400. [PubMed: 2070077]
59. Bajaj MS, Kuppuswamy MN, Saito H, Spitzer SG, Bajaj SP. Cultured normal human hepatocytes do not synthesize lipoprotein-associated coagulation inhibitor: evidence that endothelium is the principal site of its synthesis. Proc Natl Acad Sci U S A 1990; 87: 8869–73. [PubMed: 2247459]
60. Mast AE. Tissue Factor Pathway Inhibitor: Multiple Anticoagulant Activities for a Single Protein. Arterioscler Thromb Vasc Biol 2016; 36: 9–14. [PubMed: 26603155]
61. Ott I, Miyagi Y, Miyazaki K, Heeb MJ, Mueller BM, Rao LV, Ruf W. Reversible regulation of tissue factor-induced coagulation by glycosyl phosphatidylinositol-anchored tissue factor pathway inhibitor. Arterioscler Thromb Vasc Biol 2000; 20: 874–82. [PubMed: 10712416]
62. Mast AE, Acharya N, Malecha MJ, Hall CL, Dietzen DJ. Characterization of the association of tissue factor pathway inhibitor with human placenta. Arterioscler Thromb Vasc Biol 2002; 22: 2099–104. [PubMed: 12482841]
63. Maroney SA, Cunningham AC, Ferrel J, Hu R, Haberichter S, Mansbach CM, Brodsky RA, Dietzen DJ, Mast AE. A GPI-anchored co-receptor for tissue factor pathway inhibitor controls its intracellular trafficking and cell surface expression. J Thromb Haemost 2006; 4: 1114–24. [PubMed: 16689766]

64. Hamamoto T, Yamamoto M, Nordfang O, Petersen JG, Foster DC, Kisiel W. Inhibitory properties of full-length and truncated recombinant tissue factor pathway inhibitor (TFPI). Evidence that the third Kunitz-type domain of TFPI is not essential for the inhibition of factor VIIa-tissue factor complexes on cell surfaces. J Biol Chem 1993; 268: 8704–10. [PubMed: 8473315]

65. Valentin S, Reutlingsperger CP, Nordfang O, Lindhout T. Inhibition of factor X activation at extracellular matrix of fibroblasts during flow conditions: a comparison between tissue factor pathway inhibitor and inactive factor VIIa. Thromb Haemost 1995; 74: 1478–85. [PubMed: 8772224]

66. Lindhout T, Salemink I, Valentin S, Willems GM. Tissue factor pathway inhibitor: regulation of its inhibitory activity by phospholipid surfaces. Haemostasis 1996; 26(Suppl 4): 89–97. [PubMed: 8979115]

ESSENTIALS

- Mouse models are often used to define roles of tissue factor pathway inhibitor (TFPI) in man.
- TFPI isoform-specific KOs reveals unexpected differences between mouse and human TFPI physiology.
- Mouse plasma contains 20 times more TFPI than man, derived from TFPI, a form not found in man.
- TFPIγ null mice, expressing only TFPI isoforms α and β, may better reflect the human situation.

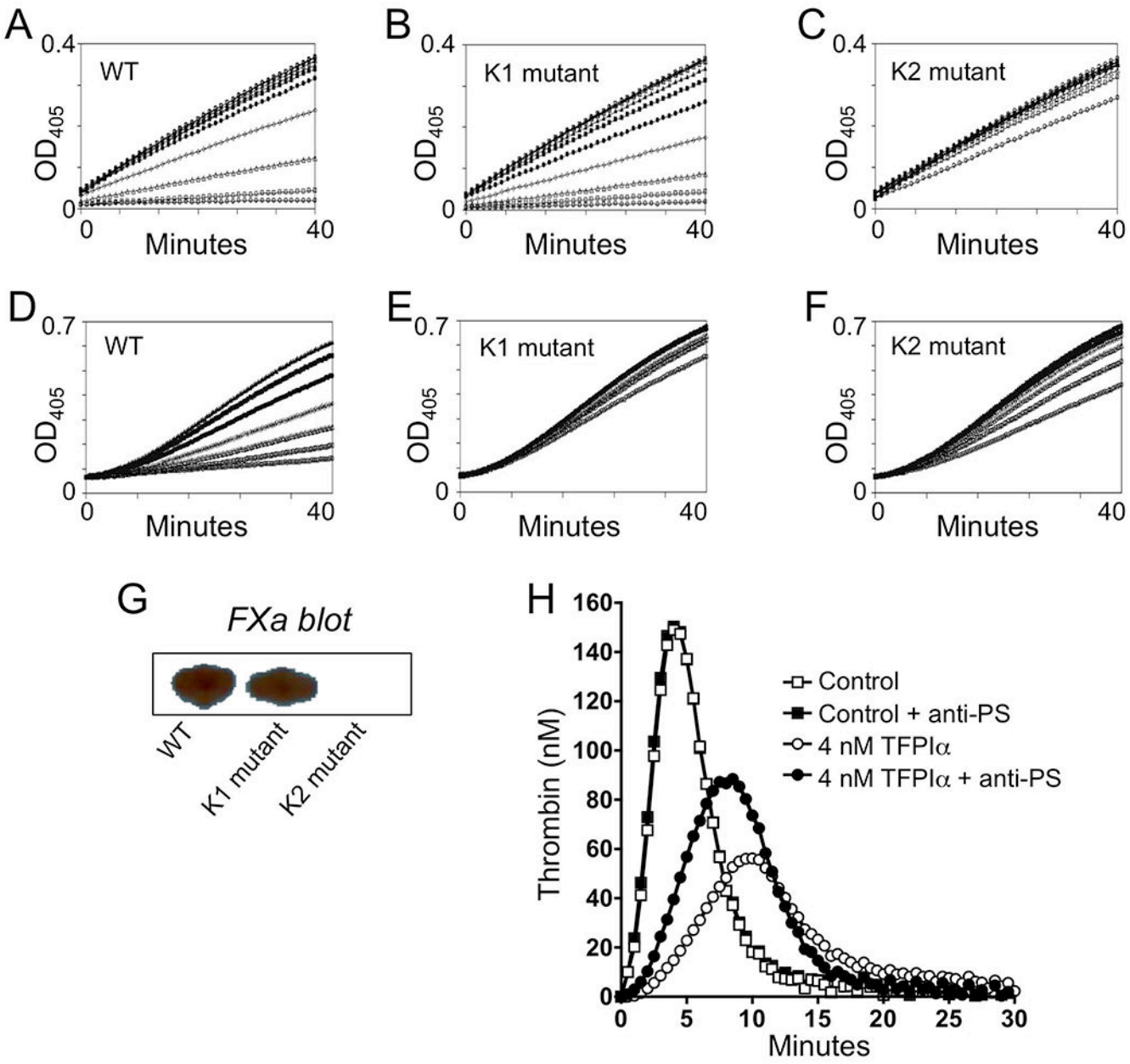

Figure 1.

Structure/function analysis of mTFPI. Recombinant mTFPI(1-157) WT (A and D), K1 P1 mutated (B and E) and K2 P1 mutated (C and F) forms were tested for effects at 0 and serial two-fold dilutions from 20 nM TFPI in a mouse FXa assay (A-C) and at 0 and serial two-fold dilutions from 2 nM TFPI in a mouse FVIIa/TF assay (D-F). (G) Bovine FXa-HRP ligand blot of WT and the K1 and K2 mutant forms of mTFPI (40 ng). (H) Effect of anti-hPS antibodies (200 ug/mL) on mTF-induced (0.4 pM final) thrombin generation in mouse plasma in the absence and presence of added rmTFPIα (4 nM).

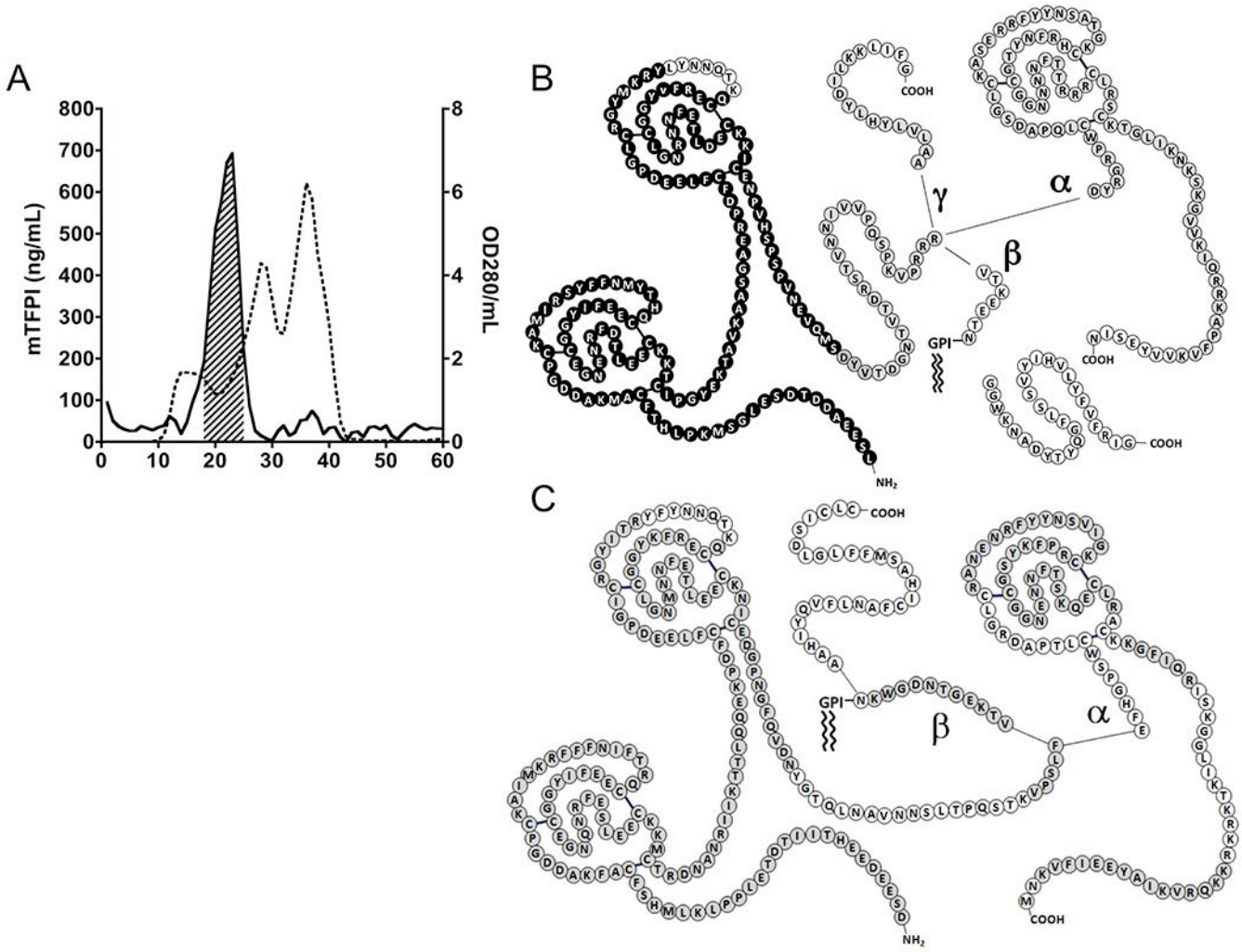

Figure 2.

Characterization of mouse and human plasma TFPI. (A) A representative Sephacryl 300 sizeexclusion chromatography of mouse plasma. Shown are mTFPI by ELISA (solid line) and protein based on OD280 (dotted line); the hash-marked area indicates the lipoprotein fractions pooled for further processing. (B) MS/MS analysis of mouse TFPI. Amino acids in black correspond to peptide spectra identified in the mouse lipoprotein-associated TFPI sample; amino acids in light gray correspond to additional peptide spectra identified in the total mouse plasma TFPI sample; and amino acids in white correspond to regions where no corresponding peptide spectra were identified in either sample. (C) MS/MS analysis of human TFPI. Amino acids in gray correspond to peptide spectra identified in the total human plasma TFPI sample; and amino acids in white correspond to regions were no corresponding peptide spectra were identified.

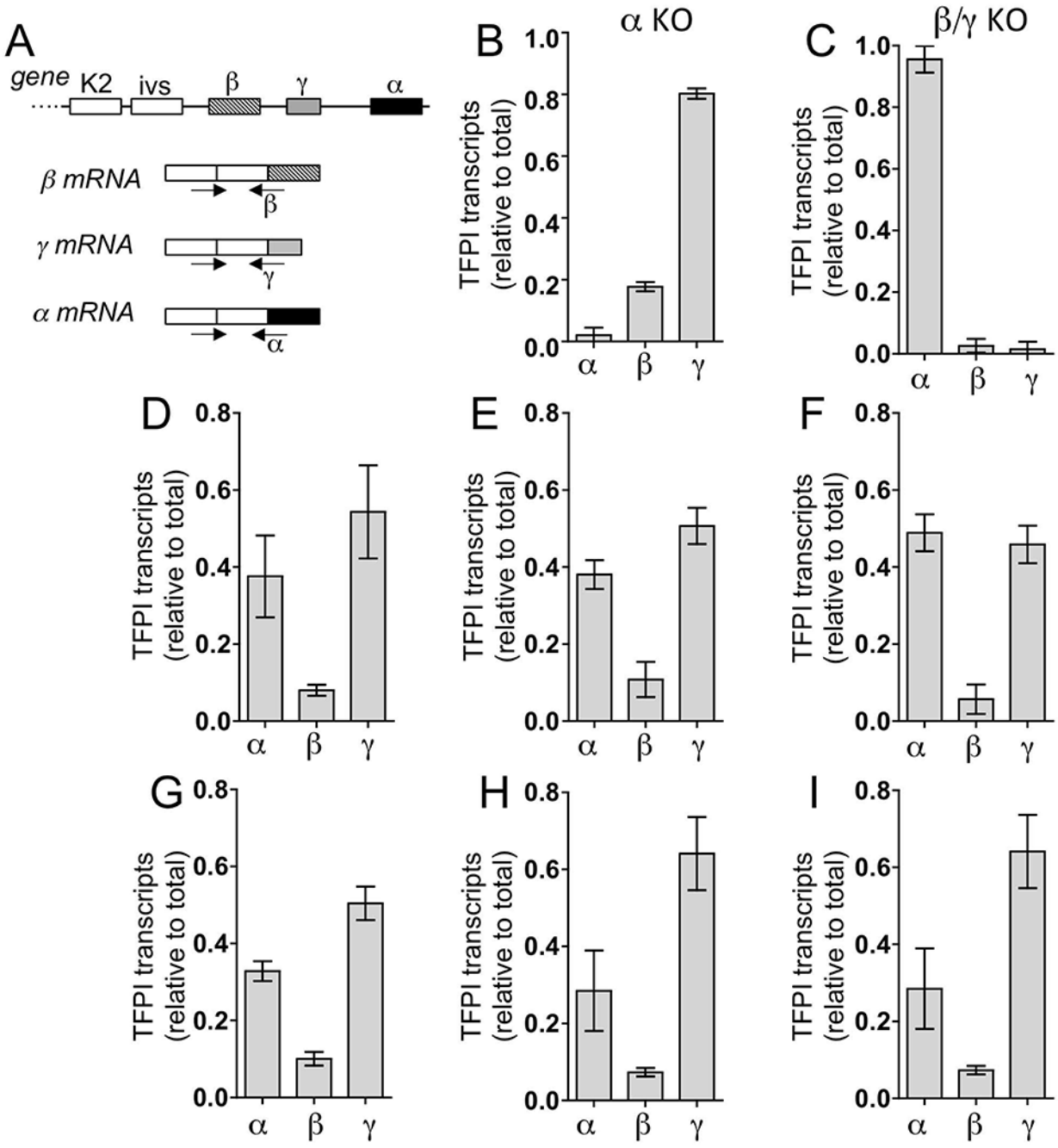

Figure 3.

Quantification of mTFPI isoform transcripts. (A) Scheme for isoform-specific amplifications. Selectivity of each RT-PCR assay is indicated by the effect of (B) α-exon deletion on TFPIα transcripts and (C) TFPIβ/γ-exon deletions on TFPI β, and γ transcripts in lung. Shown are means + SEM (n=3/group). The relative levels of each TFPI isoform transcript were determined for (D) brain; (E) heart; (F) kidney; (G) liver; (H) lung; and (I) spleen of WT mice. Shown are means + SEM (n=5/group).

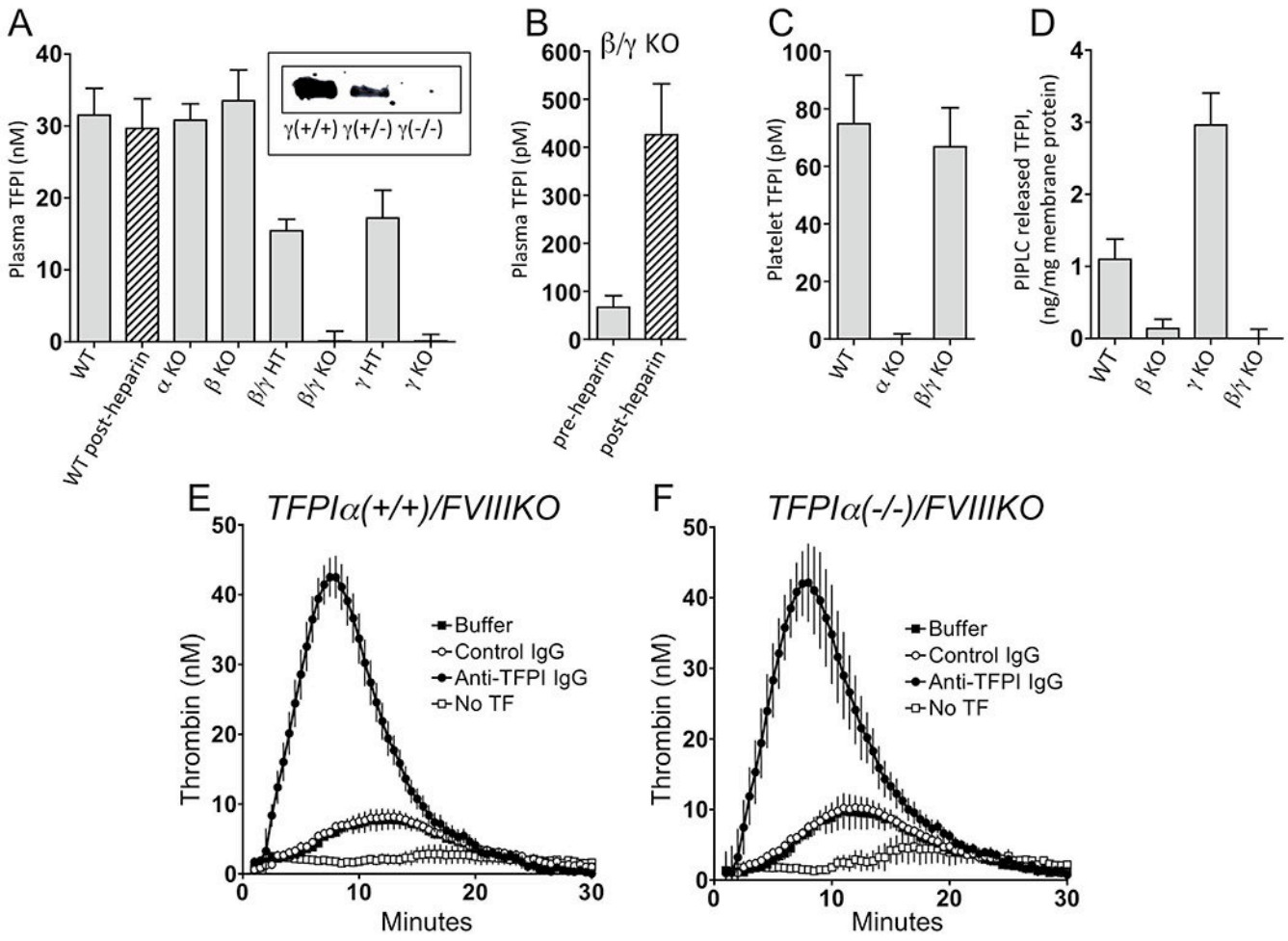

Figure 4.

Levels of TFPI in TFPI exon KO mice and anticoagulant effect of mouse plasma TFPI. (A) Plasma TFPI levels (n=5-10/group); insert is a western blot using polyclonal anti-mTFPI160 IgG-HRP of 1 uL plasma from mice with the various TFPIγ genotypes. (B) Plasma TFPI levels in TFPIβ/γ KO mice pre- and postheparin treatment (n=5). (C) Platelet-associated TFPI in mouse blood (based on 850,000 platelets/uL, n=4). (D) PIPLC released TFPl from WT, β KO, γ KO and β/γ KO liver membranes (n=3-6/group). (E) and (F) TFinduced (0.02 pM final) thrombin generation in plasmas from littermate TFPIα(+/+)/FVIIIKO mice (n=3) and TFPIα(−/−)/FVIIIKO mice (n=3), respectively. Inserts in E and F: Buffer, HSA; Control IgG (200 ug/mL); Anti-TFPI IgG, anti-mTFPI160 IgG (200 ug/mL); No TF, without TF induction or antibody treatment. Results depicted as mean + SEM in each panel.

Table 1.

Primers and probes used.

Reaction	Primers (5' to 3')	DNA size (base pairs)	
Mouse genotyping		**WT**	**KO**
WT α	For: TCCCCTGCGCCACTCTGCACTTGCTT	452	none
KO α	For: TCGATTCCAAACCAGTGTCCTACTATA	(2543)	593
common	Rev: ATTGTTGACGGAAATGTAGAAAGCTTC		
common	For: TGTGCTTTGCGGTAGGGCTTCTGTGTA		
WT β/γ	Rev: GCTTAGGCGCTCCTTTCTCA	1003	none
KO β/γ	Rev: TTCTGGGCAGCAGATCTTTCCTGCTCT	(3863)	643
WT β	For: TGTGCTTTGCGGTAGGGCTTCTGTGTA	1003	459
and KO β	Rev: GCTTAGGCGCTCCTTTCTCA		
WT γ	For: CCTTGCTTCTATACATCATCTCTTAACAGC	153	none
KO γ	For: CCTTGCTTCTATACATCATCTCTTAATAT	none	154
common	Rev: GCTTAGGCGCTCCTTTCTCA		
RT-PCR for mouse TFPI isoform transcripts			
probe	FAM-CATCGTGGTTCCCCAGTCTC-MGBNFQ		
common	For: CTGTGAGAATCCAGTCCACTCC		
α primer	Rev: GCCACGATAATCCCGACG		
β primer	Rev: TCTTCTTTTGTAACCCGACGC		
γ primer	Rev: TACCAAGGCAGCCCGAC		
RT-PCR for human γ sequence in transcripts			
	For: CAAGAACATTTGTGAAGATGGTCC		
	Rev: ATAAAGCTGATGTAGTTCCAAGGC		

Table 2.

TFPI isoform KO sequences flanking the exon deletions or disruption.

Exon targeted	Flanking sequences
α	5'-TAGGATTCTGCTTTATTCAGAAGAC-(1950 base deletion)-AGCACTTTCCTTG GGTAGGTAACAG-3'
β/γ	5'-GATATTCGCTG GCCCACTCTTCCTA-(3220 base deletion)-TTGCCCATAGGTTTTGTGTGTGTAT-3'
β	5'-CCTGAAACTGATATTCGCTGGCCCA-(556 base-deletion plus GCGTTCA)-TGGAGAAAAGTTAATTATTTTCCAA-3'
γ	5'-CATCTCTTAA**CAG/C**TGCCTTGGTACTGT-3' (splice site changed to) 5'-CATCTCTTAA***TAT***TGC**A**TTGGTACTGT-3'

Table 3.

Mouse TFPIγ exon orthologs.

Species	3’ intron Splice	Predicted Amino Acid Sequences (Alignment with Rat Sequence)
Cat	TAG	**AALGL**HQ**LYDI**WE**K**NLQIDFKSPLATQSDIWKVIWVPETHFLLPD–CIQHMPYWPDSTYM
Dog	TAG	**AALGL**HQ**LYDIL**E**K**SSDRLQKPAGNSASHLVSDYVFDLLLTASWQ–PLGQGKMIDYHFANHL
Rabbit	CAG	GV**LGL**HQC**YDIL**GNKSLVNFENLLPTNLIVAL
Mouse	CAG	**AAL**V**LYHLYDILKKLIFG**
Rat	CAG	**AALGLYHLYDILKKLIFG**
Hamster	CAG	V**ALGL**H**HLYDILKKLIFG**
Squirrel	CAG	**AALGL**HQ**LYDIL**E**K**I**IFG**
Night Monkey	GAG	**AAL**E**L**HQ**LY**N**IL**GGKNLWVDLKSY
Macaque	GAG	**A**NWEQHQ**LYDIL**GGKK**F**R
Orangutan	GAG	G**AL**E**L**HQ**LYDIL**GGRK**F**R
Man	GAG	G**AL**E**L**HQ**LYDIL**GGRK**F**R

Table 4.

Genotype distributions of offspring at weaning.

	TFPI(+/−) × TFPI(+/−)			
Isoform deletion	**TFPI(+/+)**	**TFPI(+/−)**	**TFPI(−/−)**	**P value** *
α	62	136	48	0.1141
β/γ	28	45	25	0.6581
β	21	34	21	0.6564
γ	7	18	12	0.502

* Two tailed for Chi square test expecting 1:2:1 Mendelian ratios.